Optica Applicata, Vol. XLVIII, No. 2, 2018
DOI: 10.5277/oa180212

Changes in the polarization states of random electromagnetic vortex beams propagating in biological tissues

MEILING DUAN[*,**], YUNGUANG WU[**], NINGNING SU

Department of Physics, North University of China, Taiyuan 030051, China

[*]Corresponding author: meilingduan@nuc.edu.cn

[**]These authors contributed equally to this work and should be considered co-first authors.

The changes in the on-axis polarization state of random electromagnetic Gaussian Schell-model vortex beams propagating in biological tissues have been studied. In different media propagation, the bigger C_n^2 is, the earlier the appearance of the inflexion points in the on-axis degree of the polarization $P(0, 0, z)$ is. As the propagation distance increases, the values of the on-axis orientation angle $\theta(0, 0, z)$ undergo several processes: at the beginning they are positive, then gradually increase to the maximum, jump to a negative value, finally tend to a fixed value. The bigger C_n^2 corresponds to previous jumping position. In the entire propagation, the values of the on-axis ellipticity $\varepsilon(0, 0, z)$ are larger than the initial one. There exists a phenomenon that the values of $P(0, 0, z)$, $\theta(0, 0, z)$ and $\varepsilon(0, 0, z)$ keep their extremes in a length of propagation distances for the far infrared beams. The maximum of $P(0, 0, z)$ is the smallest and the jumping range of $\theta(0, 0, z)$ is the largest for the ultraviolet beams. Compared with $\sigma_{yy} > \sigma_{xx}$, the changes in magnitudes in $P(0, 0, z)$ are more obvious when $\sigma_{yy} < \sigma_{xx}$, the changes in $\theta(0, 0, z)$ are just the reverse for $\sigma_{yy} < \sigma_{xx}$.

Keywords: random electromagnetic vortex beam, biological tissue, the state of polarization.

1. Introduction

The propagation properties of a laser beam passing through the media are closely connected with the optical properties of the media. Thus the beams propagation is one of important research fields in optics, and the optical characteristics changes of the media can be reflected by the propagation properties changes of a laser beam through the media, which becomes a significant project in optical medicine [1–3]. The polarization of light is the basic property of light, which is a manifestation of correlations involving components of the fluctuating electric field at a single point or two points [4]. In 2005 WESTPHAL and HELL pointed out that the orientation of the linear molecular transition dipole is of great effect on the spatial resolution in stimulated emission depletion fluorescence microscopy [5], so it is important to know the state of polarization of the

polarized part of the beam at a point and its changes on propagation. In 1996 SCHMITT and KUMAR reported that the power spectrum model of mammalian tissue can be described mathematically by a model that resembles the classical Kolmogorov model of atmospheric turbulence [6]. Based on the unified theory of coherence and polarization [4], some works have been devoted to the changes in the state of polarization of random electromagnetic beams in biological tissues. Such as the change in the state of polarization of isotropic random electromagnetic beams passing through biological tissues [7, 8], the change in the degree of polarization of anisotropic random electromagnetic beams passing through biological tissues [9], and so on. However, lots of researches concern the non-vortex beams, those referring to the change in the state of polarization of vortex beams are scarce.

The vortex beam is a singular beam endowed with the screw wavefront dislocations, topological charge and optical vortex, which has attracted attention and found extensive applications in optical communications, quantum information and entanglement, and microparticle manipulation and trapping [10–16]. The influence of both the topological charge and the correlation length of the beam on the degree of polarization of stochastic electromagnetic vortex beams has been studied [17]. In this paper, based on the extended Huygens–Fresnel principle, the analytical expressions of the cross-spectral density matrix elements for random electromagnetic Gaussian Schell-model (GSM) vortex beam propagating in biological tissues are derived. The dependence of the changes in the on-axis polarization state of random electromagnetic GSM vortex beams propagating in biological tissues has been studied by means of numerical calculations, including the structure constant of the refractive index C_n^2 of biological tissues, the wavelength λ, the spatial correlation length σ_{yy} of beams, and the propagation distance z.

2. Theoretical model

The cross-spectral density matrix of random electromagnetic vortex beams at the source plane $z = 0$ is expressed as [18]

$$\mathbf{W}(\mathbf{s}_1, \mathbf{s}_2, 0) = \begin{bmatrix} W_{xx}(\mathbf{s}_1, \mathbf{s}_2, 0) & W_{xy}(\mathbf{s}_1, \mathbf{s}_2, 0) \\ W_{yx}(\mathbf{s}_1, \mathbf{s}_2, 0) & W_{yy}(\mathbf{s}_1, \mathbf{s}_2, 0) \end{bmatrix} \tag{1}$$

where

$$W_{ij}(\mathbf{s}_1, \mathbf{s}_2, 0) = \langle E_i^*(\mathbf{s}_1, 0) E_j(\mathbf{s}_2, 0) \rangle, \quad i, j = x, y \tag{2}$$

where E_x and E_y denote the two components of the electric field; $\mathbf{s}_l \equiv (s_{lx}, s_{ly})$ ($l = 1$ and 2) is the two-dimensional position vector at the source plane $z = 0$. The asterisk and angle brackets stand for the complex conjugate and ensemble average, respectively.

The elements $W_{ij}(\mathbf{s}_1, \mathbf{s}_2, 0)$ of the cross-spectral density matrix of random electromagnetic GSM vortex beams at the source plane are expressed as [19]

$$W_{ij}(\mathbf{s}_1, \mathbf{s}_2, 0) = A_i A_j B_{ij}\left[s_{1x}s_{2x} + s_{1y}s_{2y} + i\,\mathrm{sgn}(m)s_{1x}s_{2y} - i\,\mathrm{sgn}(m)s_{2x}s_{1y}\right]^{|m|} \times \exp\left(-\frac{\mathbf{s}_1^2 + \mathbf{s}_2^2}{w_0^2}\right)\exp\left(-\frac{(\mathbf{s}_1 - \mathbf{s}_2)^2}{2\sigma_{ij}^2}\right) \tag{3}$$

where A_i is the amplitude of the electric field-vector component, E_i, and B_{ij} are correlation coefficients between two components E_i and E_j, w_0 is the waist width, σ_{ij} is related to the spatial correlation length; sgn(m) denotes the sign function; m specifies the topological charge, and in the following we take $m = +1$. For $m = 0$, Eq. (3) reduces to those of random electromagnetic GSM vortex-free beams,

$$W'_{ij}(\mathbf{s}_1, \mathbf{s}_2, 0) = A_i A_j B_{ij}\exp\left(-\frac{\mathbf{s}_1^2 + \mathbf{s}_2^2}{w_0^2}\right)\exp\left(-\frac{(\mathbf{s}_1 - \mathbf{s}_2)^2}{2\sigma_{ij}^2}\right) \tag{4}$$

Based on the extended Huygens–Fresnel principle [20], the elements of cross-spectral density matrix of random electromagnetic GSM vortex beams propagating through biological tissue can be expressed as

$$W_{ij}(\boldsymbol{\rho}_1, \boldsymbol{\rho}_2, z) = \left(\frac{k}{2\pi z}\right)^2 \iint \mathrm{d}^2\boldsymbol{\rho}_1 \iint \mathrm{d}^2\boldsymbol{\rho}_2\, W_{ij}(\mathbf{s}_1, \mathbf{s}_2, 0) \times \exp\left\{-\frac{ik}{2z}\left[(\boldsymbol{\rho}_1 - \mathbf{s}_1)^2 - (\boldsymbol{\rho}_2 - \mathbf{s}_2)^2\right]\right\}\langle \exp[\psi^*(\boldsymbol{\rho}_1, \mathbf{s}_1) + \psi(\boldsymbol{\rho}_2, \mathbf{s}_2)]\rangle \tag{5}$$

where the $\boldsymbol{\rho}_1$ and $\boldsymbol{\rho}_2$ is the position vector at the z plane, the relationship between the wave number k and the wavelength λ is $k = 2\pi/\lambda$, ψ denotes the random part of the complex phase of a spherical wave propagating through the biological tissue, and $\langle\cdot\rangle$ implies the averaging over the ensemble of the statistical realizations of the random medium and can be written as [21]

$$\langle \exp[\psi^*(\boldsymbol{\rho}_1, \mathbf{s}_1) + \psi(\boldsymbol{\rho}_2, \mathbf{s}_2)]\rangle = \exp\left\{-4\pi^2 k^2 z \int_0^1 \mathrm{d}t \int_0^\infty \mathrm{d}\kappa\, \kappa \Phi(\kappa)\left[1 - J_0\left(\left|t(\boldsymbol{\rho}_1 - \boldsymbol{\rho}_2) + (1-t)(\mathbf{s}_1 - \mathbf{s}_2)\right|\kappa\right)\right]\right\} \tag{6}$$

where J_0 is the zero-order Bessel function, and $\Phi(\kappa)$ is known as the power spectrum of the index of refraction fluctuations. As for a variety of mammalian tissues such as human skin, the expression of $\Phi(\kappa)$ is written as [6]

$$\Phi(\kappa) = \frac{4\pi\langle\delta n^2\rangle L_0^2(\zeta-1)}{(1+\kappa^2 L_0^2)^{\zeta}} \tag{7}$$

where L_0 is the outer scale of the refractive-index size, the parameter ζ is related to the fractal dimension of the tissue and is an indication of the classical turbulent behavior of tissue, and $\langle\delta n^2\rangle$ is the ensemble averaged variance of the refractive index.

In Eq. (6), the expansion of $J_0(x)$ can be expressed as [9]

$$J_0(x) = \sum_0^m \frac{(-1)^m (x/2)^{2m}}{(m!)^2}, \qquad |x| < \infty \tag{8}$$

When we will take the front two items as its approximate expression, then the expression of $\langle\exp[\psi^*(\boldsymbol{\rho}_1, \mathbf{s}_1) + \psi(\boldsymbol{\rho}_2, \mathbf{s}_2)]\rangle$ can be rewritten as

$$\langle\exp[\psi^*(\boldsymbol{\rho}_1, \mathbf{s}_1) + \psi(\boldsymbol{\rho}_2, \mathbf{s}_2)]\rangle \cong -\frac{1}{\rho_0^2}\left[(\boldsymbol{\rho}_1-\boldsymbol{\rho}_2)^2 + (\boldsymbol{\rho}_1-\boldsymbol{\rho}_2)(\mathbf{s}_1-\mathbf{s}_2) + (\mathbf{s}_1-\mathbf{s}_2)^2\right] \tag{9}$$

where

$$\rho_0 = 0.22(C_n^2 k^2 z)^{-1/2} \tag{10}$$

means the coherence length of a spherical wave propagating through turbulence, C_n^2 is the structure constant of refractive index describing the strength of biological tissue turbulence, whose expression is

$$C_n^2 = \frac{\langle\delta n^2\rangle}{L_0^2(2-\zeta)} \tag{11}$$

where L_0 is the outer scale of refractive-index size, ζ is related to the fractal dimension of biological tissues, $\langle\delta n^2\rangle$ is the ensemble-averaged variance of the refractive index. $C_n^2 = 0$ for the free space. In order to facilitate the calculation, two variables of integration are introduced:

$$\mathbf{u} = \frac{\mathbf{s}_1+\mathbf{s}_2}{2}, \qquad \mathbf{v} = \mathbf{s}_1-\mathbf{s}_2 \tag{12}$$

and substituting Eqs. (3) and (9) into Eq. (5), we obtain

$$W_{ij}(\boldsymbol{\rho}_1, \boldsymbol{\rho}_2, z) = A_i A_j B_{ij} \left(\frac{k}{2\pi z}\right)^2 \exp\left[-\frac{ik}{2z}(\boldsymbol{\rho}_1^2 - \boldsymbol{\rho}_2^2)\right]$$

$$\times \exp\left[-\frac{1}{\rho_0^2}(\boldsymbol{\rho}_1^2 - \boldsymbol{\rho}_2^2)\right] \iint \mathrm{d}^2 u \iint \mathrm{d}^2 v \left[\left(\mathbf{u}^2 - \frac{\mathbf{v}^2}{4}\right) - i(u_x v_y - u_y v_x)\right]$$

$$\times \exp\left[-\frac{2}{w_0^2}u_x^2 - \frac{2}{w_0^2}u_y^2\right] \exp\left[-a_{ij}v_x^2 - a_{ij}v_y^2\right] \exp\left[-\frac{ik}{z}\mathbf{u}(\boldsymbol{\rho}_2 - \boldsymbol{\rho}_1)\right]$$

$$\times \exp\left[-\frac{ik}{2z}\mathbf{v}(\boldsymbol{\rho}_2 + \boldsymbol{\rho}_1)\right] \exp\left[-\frac{ik}{z}\mathbf{u}\mathbf{v}\right] \exp\left[-\frac{1}{\rho_0^2}\mathbf{v}(\boldsymbol{\rho}_1 - \boldsymbol{\rho}_2)\right]$$

$$\times \exp\left[\frac{ik}{2z}\mathbf{v}(\boldsymbol{\rho}_2 + \boldsymbol{\rho}_1)\right] \exp\left[-\frac{ik}{z}\mathbf{u}\mathbf{v}\right] \exp\left[-\frac{1}{\rho_0^2}\mathbf{v}(\boldsymbol{\rho}_1 - \boldsymbol{\rho}_2)\right] \tag{13}$$

where

$$a_{ij} = \frac{1}{2w_0^2} + \frac{1}{2\sigma_{ij}^2} + \frac{1}{\rho_0^2} \tag{14}$$

Recalling the integral formula [22]

$$\int x^n \exp(-px^2 + 2qx)\mathrm{d}x = n! \exp\left(\frac{q^2}{p}\right)\sqrt{\frac{\pi}{p}}\left(\frac{q}{p}\right)^n \sum_{k=0}^{E\left[\frac{n}{2}\right]} \frac{1}{(n-2k)!k!}\left(\frac{p}{4q^2}\right)^k \tag{15}$$

the analytical expression of the cross-spectral density function of the GSM vortex beams propagating through the biological tissue can be obtained by tedious and straightforward integral calculations for Eq. (13):

$$W_{ij}(\boldsymbol{\rho}_1, \boldsymbol{\rho}_2, z)$$

$$= A_i A_j B_{ij} \exp\left[-\frac{ik}{2z}(\boldsymbol{\rho}_1^2 - \boldsymbol{\rho}_2^2) - \frac{1}{\rho_0^2}(\boldsymbol{\rho}_1 - \boldsymbol{\rho}_2)^2\right]\left[M_1 - M_2 - M_3 + M_4\right] \tag{16}$$

where

$$M_1 = \frac{k^2 b_x b_y}{4z^2 a_{ij} c}\left(\frac{1}{c} + \frac{d_x^2 + d_y^2}{c^2}\right)\exp\left(\frac{d_x^2 + d_y^2}{c}\right) \tag{17a}$$

$$M_2 = \frac{k^2 w_0^2}{32 z^2 f}\left(\frac{1}{f} + \frac{g_x^2 + g_y^2}{f^2}\right)\exp\left(\frac{g_x^2 + g_y^2}{f^2}\right) \times \exp\left\{\frac{w_0^2}{8}\left[-\frac{k^2}{z^2}(\rho_{1x} - \rho_{2x})^2 - \frac{k^2}{z^2}(\rho_{1y} - \rho_{2y})^2\right]\right\} \tag{17b}$$

$$M_3 = \frac{i k^2 w_0 g_y d_x b_x}{4z^2\sqrt{2a_{ij} f^3 c^3}}\exp\left[-\frac{w_0^2 k^2}{8z}(\rho_{1y} - \rho_{2y})^2\right]\exp\left(\frac{g_y^2}{f} + \frac{d_x^2}{c}\right) \tag{17c}$$

$$M_4 = \frac{i k^2 w_0 g_x d_y b_y}{4z^2\sqrt{2a_{ij} f^3 c^3}}\exp\left[-\frac{w_0^2 k^2}{8z}(\rho_{1x} - \rho_{2x})^2\right]\exp\left(\frac{g_x^2}{f} + \frac{d_y^2}{c}\right) \tag{17d}$$

$$c = \frac{2}{w_0^2} + \frac{k^2}{4z^2 a_{ij}} \tag{17e}$$

$$f = a_{ij} + \frac{w_0^2 k^2}{8z^2} \tag{17f}$$

$$d_x = \frac{k^2}{8a_{ij} z^2}(\rho_{1x} + \rho_{2x}) + \frac{ik}{2z}\left(1 + \frac{1}{2a_{ij}\rho_0^2}\right)(\rho_{1x} - \rho_{2x}) \tag{17g}$$

$$g_x = \frac{ik}{4z}(\rho_{1x} + \rho_{2x}) + \frac{1}{2}\left(\frac{w_0^2 k^2}{4z^2} - \frac{1}{\rho_0^2}\right)(\rho_{1x} - \rho_{2x}) \tag{17h}$$

$$b_x = \exp\left\{\frac{1}{4a_{ij}}\left[\frac{ik}{2z}(\rho_{1x} + \rho_{2x}) - \frac{1}{\rho_0^2}(\rho_{1x} - \rho_{2x})\right]^2\right\} \tag{17i}$$

According to the symmetry, d_y, g_y and b_y can be obtained by the replacement of ρ_{1x} and ρ_{2x} with ρ_{1y} and ρ_{2y}, respectively.

Based on the unified theory of polarization and coherence, the degree of polarization $P(\boldsymbol{\rho}_1, \boldsymbol{\rho}_2, z)$ of the random electromagnetic GSM vortex beam propagating through the biological tissues can be expressed as [18, 23]

$$P(\boldsymbol{\rho}_1, \boldsymbol{\rho}_2, z) = \sqrt{1 - \frac{4\mathrm{Det}[\mathbf{W}(\boldsymbol{\rho}_1, \boldsymbol{\rho}_2, z)]}{\mathrm{Tr}[\mathbf{W}(\boldsymbol{\rho}_1, \boldsymbol{\rho}_2, z)]^2}} \tag{18}$$

where Det and Tr denote the determinant of the matrix and the trace of the matrix, respectively.

The orientation angle $\theta(\boldsymbol{\rho}_1, \boldsymbol{\rho}_2, z)$ is made by the major axis of the polarization ellipse with the x-direction, and the expression can be written as [18]

$$\theta(\boldsymbol{\rho}_1, \boldsymbol{\rho}_2, z) = \frac{1}{2}\arctan\left(\frac{2\mathrm{Re}[W_{xy}(\boldsymbol{\rho}_1, \boldsymbol{\rho}_2, z)]}{W_{xx}(\boldsymbol{\rho}_1, \boldsymbol{\rho}_2, z) - W_{yy}(\boldsymbol{\rho}_1, \boldsymbol{\rho}_2, z)}\right) \tag{19}$$

The ellipticity $\varepsilon(\boldsymbol{\rho}_1, \boldsymbol{\rho}_2, z)$ can be used to describe the shape of the polarization ellipse, and the formula is given as [18]

$$\varepsilon(\boldsymbol{\rho}_1, \boldsymbol{\rho}_2, z) = A_{\mathrm{minor}}/A_{\mathrm{major}}, \qquad 0 \le \varepsilon \le 1 \tag{20}$$

where A_{major} and A_{minor} are the major and minor semi-axis of the polarization ellipse, respectively, and can be expressed as

$$A^2_{\mathrm{major}}(\boldsymbol{\rho}_1, \boldsymbol{\rho}_2, z) = \frac{\sqrt{(W_{xx} - W_{yy})^2 + 4|W_{xy}|^2} + \sqrt{(W_{xx} - W_{yy})^2 + 4|\mathrm{Re}(W_{xy})|^2}}{2} \tag{21a}$$

$$A^2_{\mathrm{minor}}(\boldsymbol{\rho}_1, \boldsymbol{\rho}_2, z) = \frac{\sqrt{(W_{xx} - W_{yy})^2 + 4|W_{xy}|^2} - \sqrt{(W_{xx} - W_{yy})^2 + 4|\mathrm{Re}(W_{xy})|^2}}{2} \tag{21b}$$

When $\boldsymbol{\rho}_1 = \boldsymbol{\rho}_2 = 0$, Eqs. (18)–(20) reduce to the on-axis state of polarization $P(0, 0, z)$, $\theta(0, 0, z)$ and $\varepsilon(0, 0, z)$ of the random electromagnetic GSM vortex beam.

3. Numerical calculations and analysis

It is important to know the state of polarization of the beam at a point and its changes during the propagation. We select the upper dermis of human, the deep dermis of mouse and the intestinal epithelium of mouse as the specimens of numerical calculations, and investigate the changes in the on-axis state of polarization of the random electromagnetic GSM vortex beam passing through the biological tissues. The corresponding changes in free space also have been discussed. According to Eq. (11) and the data in [6], $C_n^2 = 0.44 \times 10^{-3}$ μm^{-1} in upper dermis of human, $C_n^2 = 0.22 \times 10^{-3}$ μm^{-1} in deep dermis of mouse, $C_n^2 = 0.06 \times 10^{-3}$ μm^{-1} in intestinal epithelium of mouse and $C_n^2 = 0$ in free space have been obtained.

Figure 1 shows the changes in the on-axis degree of polarization $P(0, 0, z)$, the on-axis orientation angle $\theta(0, 0, z)$, the on-axis ellipticity $\varepsilon(0, 0, z)$ of the random electromagnetic GSM vortex beam passing through the biological tissues with the propagation distance for different constant of the refractive index C_n^2 of the structure. The calculation parameters are $A_x = A_y = 0.5^{1/2}$, $B_{xx} = B_{yy} = 1$, $B_{xy} = B_{yx}^* = 0.3\exp(i\pi/3)$, $\sigma_{xx} = 0.15$ μm, $\sigma_{yy} = 0.225$ μm, $\sigma_{xy} = \sigma_{yx} = 0.25$ μm, $w_0 = 2$ μm, $\lambda = 0.6328$ μm, which satisfied the conditions in [24]. From Fig. 1 we see that the propagation media have no effect on the changes in $P(0, 0, z)$, $\theta(0, 0, z)$ and $\varepsilon(0, 0, z)$ at the beginning. With the increment of the propagation distance z, the values of $P(0, 0, z)$ firstly decrease and again increase to maximum, the bigger is the C_n^2, the stronger is the biological tissue turbulence, the earlier is the appearance of the inflexion points in the on-axis degree of the polarization $P(0, 0, z)$, the smaller is the maximum, and the shorter is the corresponding propagation distance. Finally $P(0, 0, z)$ keep the maximum in the free space, whereas it gradually decrease until it tends to a fixed value in the biological tissues. As the propagation distance increases, the values of $\theta(0, 0, z)$ undergo several processes: at the beginning they are positive, then gradually increase to the maximum, next jump to a negative value, and finally tend to a fixed value. Bigger C_n^2 corresponds

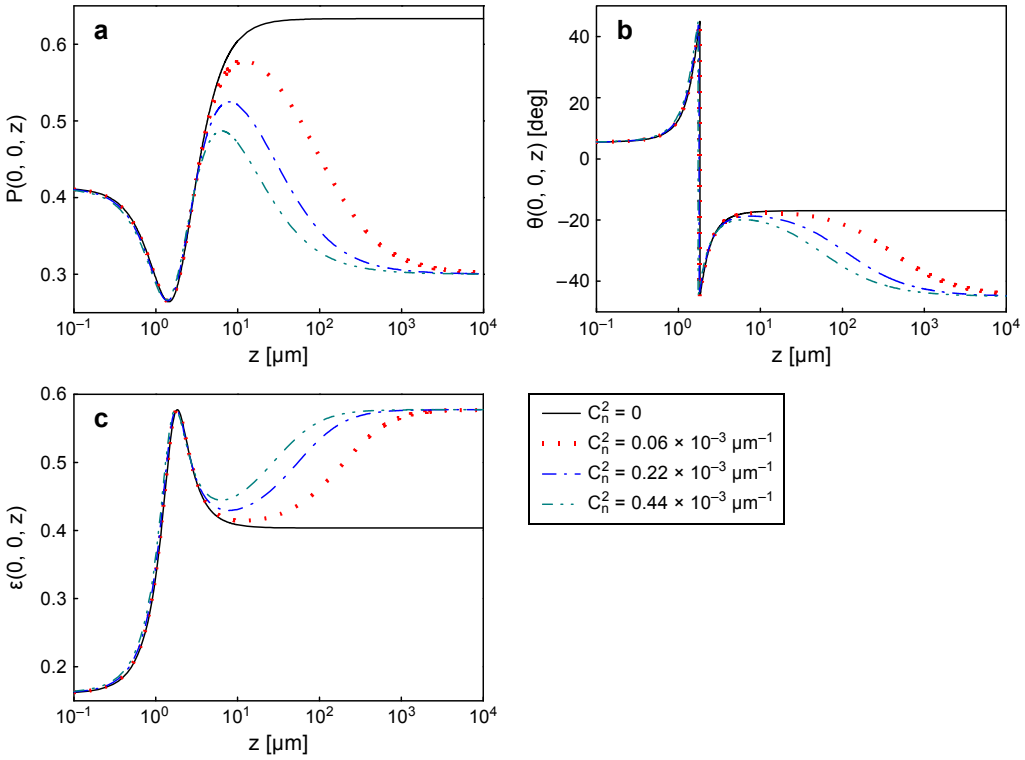

Fig. 1. The changes in the random electromagnetic GSM vortex beam with the propagation distance z in the on-axis (**a**) degree of polarization $P(0, 0, z)$, (**b**) orientation angle $\theta(0, 0, z)$ and (**c**) ellipticity $\varepsilon(0, 0, z)$ for the different structure constant of refractive index C_n^2.

to previous jumping position, for example, the jumping position of $C_n^2 = 0$, 0.06×10^{-3}, 0.22×10^{-3}, and 0.44×10^{-3} μm^{-1} is 1.84, 1.82, 1.79, and 1.74 μm, respectively. In the entire propagation, the values of $\varepsilon(0, 0, z)$ are larger than the initial one, which indicates that the propagation can enhance the on-axis ellipticity of beams.

The changes in the on-axis degree of polarization $P(0, 0, z)$, the on-axis orientation angle $\theta(0, 0, z)$, the on-axis ellipticity $\varepsilon(0, 0, z)$ of the random electromagnetic GSM vortex beam passing the upper dermis of human have been plotted with the propagation distance for different wavelength λ in Fig. 2. The calculation parameter is $C_n^2 = 0.44 \times 10^{-3}$ μm^{-1}, the other parameters are same as in Fig. 1. Herein $\lambda = 0.325$, 0.6328, and 10 μm denote the ultraviolet, visible, far infrared lights, respectively. The beams of 0.325 and 0.6328 μm can be generated by He-Cd laser and He-Ne laser, respectively, and the beam of 10 μm is so similar to the wave emitted by the biological tissue that it is named as "the life light wave". As suggested in Fig. 2, the initial values of $P(0, 0, z)$, $\theta(0, 0, z)$ and $\varepsilon(0, 0, z)$ have nothing to do with the wavelength λ. With the propagation distances increasing, the bigger λ is, the earlier the appearance of the inflexion points of $P(0, 0, z)$, $\theta(0, 0, z)$ and $\varepsilon(0, 0, z)$. During the propagation, the changes in $P(0, 0, z)$, $\theta(0, 0, z)$ and $\varepsilon(0, 0, z)$ display a phenomenon that the values keep the extreme in a length of

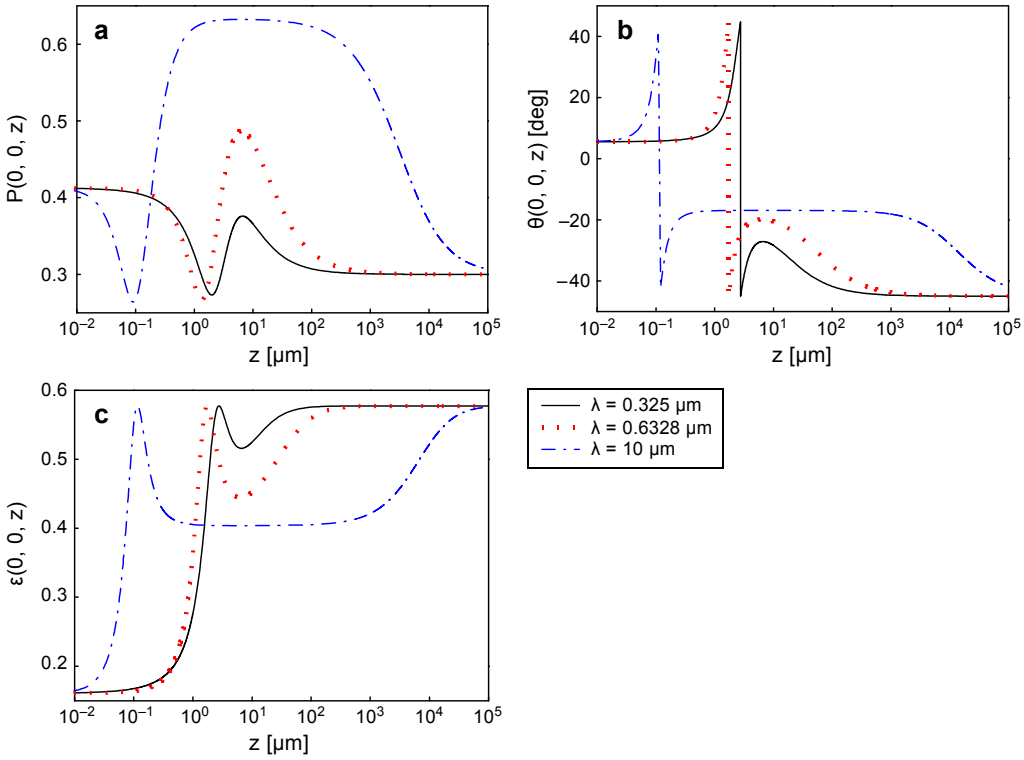

Fig. 2. The changes in the random electromagnetic GSM vortex beam propagating in upper dermis of human with the propagation distance z in the on-axis (**a**) degree of polarization $P(0, 0, z)$, (**b**) orientation angle $\theta(0, 0, z)$ and (**c**) ellipticity $\varepsilon(0, 0, z)$ for the different wavelength λ.

propagation distances for the far infrared beams. It is attributed to the fact that the far infrared light has so similar wavelength (λ = 10 μm) to the wavelength emitted by biological tissue itself that the tissue molecule resonance takes place. The maximum of $P(0, 0, z)$ is the smallest and the jumping range of $\theta(0, 0, z)$ is the largest for the ultraviolet beams. The reason can be that the protein molecules in biological tissues have strong absorption to ultraviolet light.

We plot the changes in the on-axis degree of polarization $P(0, 0, z)$, the on-axis orientation angle $\theta(0, 0, z)$, the on-axis ellipticity $\varepsilon(0, 0, z)$ of the random electromagnetic GSM vortex beam passing through the upper dermis of human with the propagation distance for the different spatial correlation length σ_{yy} in Fig. 3. The calculation parameter is $C_n^2 = 0.44 \times 10^{-3}$ μm^{-1}, $\sigma_{xx} = 0.225$ μm, the other parameters are same as in Fig. 1. It is noted that the changes in $P(0, 0, z)$, $\theta(0, 0, z)$ and $\varepsilon(0, 0, z)$ also depend on the relationship between the spatial correlation length σ_{xx} and σ_{yy}. In Fig. 3**a**, when $\sigma_{yy} < \sigma_{xx}$, the change magnitude of the curve of $P(0, 0, z)$ is more obvious than that when $\sigma_{yy} \geq \sigma_{xx}$, and the smaller σ_{yy} corresponds to the bigger extreme of $P(0, 0, z)$. From Fig. 3**b** we observe that when $\sigma_{yy} = 0.18$ and 0.2 μm, namely, $\sigma_{yy} < \sigma_{xx}$, the initial value

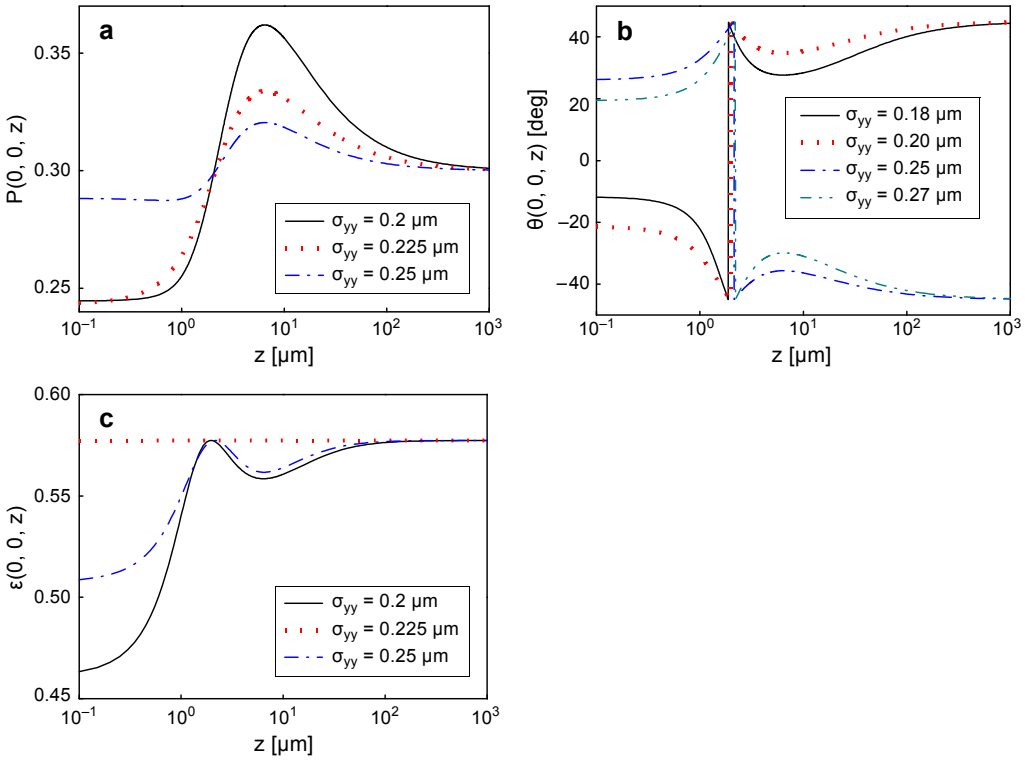

Fig. 3. The changes in the random electromagnetic GSM vortex beam propagating in upper dermis of human with the propagation distance z in the on-axis (**a**) degree of polarization $P(0, 0, z)$, (**b**) orientation angle $\theta(0, 0, z)$ and (**c**) ellipticity $\varepsilon(0, 0, z)$ for the different spatial self-correlation length σ_{yy}.

of $\theta(0, 0, z)$ is negative. With the increment of propagation distance, $\theta(0, 0, z)$ changes to the negative maximum, jump to the positive maximum, gradually decrease, and finally increase to a fixed positive one. Whereas, when $\sigma_{yy} = 0.25$ and 0.27 μm, namely, $\sigma_{yy} > \sigma_{xx}$, the changes in $\theta(0, 0, z)$ are just the reverse. The bigger the absolute value of $|\sigma_{yy} - \sigma_{xx}|$ is, the larger the change magnitude of $\theta(0, 0, z)$ is. For $\sigma_{yy} = \sigma_{xx}$ the value of $\theta(0, 0, z)$ is insignificant. It can be explained by Eqs. (16) and (19), from which $W_{yy} = W_{xx}$ can be obtained. As can be seen from Fig. 3**c**, the value of $\varepsilon(0, 0, z)$ is a fixed one from the beginning to the end when $\sigma_{yy} = \sigma_{xx}$, which can be verified by Eq. (20).

4. Conclusions

The analytical expressions of the cross-spectral density matrix elements for random electromagnetic GSM vortex beam propagating in biological tissues are derived based on the extended Huygens–Fresnel principle, and used to study the on-axis polarization state changes, including the on-axis degree of the polarization $P(0, 0, z)$, on-axis orientation angle $\theta(0, 0, z)$, and on-axis ellipticity $\varepsilon(0, 0, z)$. It is shown that in the different media propagation, the bigger C_n^2 is, the earlier the appearance of the inflexion points in $P(0, 0, z)$ is. With the increment of the propagation distance, the value of $\theta(0, 0, z)$ at the beginning is positive, again gradually increases to the maximum and jumps to negative value, and finally tends to a fixed value. The bigger C_n^2 is related to the shorter propagation distance of jumping position. The value of $\varepsilon(0, 0, z)$ firstly increases, again decreases, and finally tends to a fixed one. In the entire propagation, all values of $\varepsilon(0, 0, z)$ are larger than the initial one. During the propagation, the bigger wavelength λ is, the earlier the appearance of the inflexion points in $P(0, 0, z)$, $\theta(0, 0, z)$ and $\varepsilon(0, 0, z)$ is. Besides, the changes in $P(0, 0, z)$, $\theta(0, 0, z)$ and $\varepsilon(0, 0, z)$ display a phenomenon that their values keep the extremes in a length of propagation distances for the far infrared beams, which can be attributed to the fact that the wavelength of the far infrared light is so similar to the wave emitted by the biological tissues that the resonance with the biological tissue molecules takes place. The maximum of $P(0, 0, z)$ is the smallest and the jumping range of $\theta(0, 0, z)$ is the largest for the ultraviolet beams, which may be due to the strong absorption of the ultraviolet beam by protein molecules in biological tissues. Additionally, the changes in $P(0, 0, z)$, $\theta(0, 0, z)$ and $\varepsilon(0, 0, z)$ also depend upon the relationship between spatial correlation length σ_{yy} and σ_{xx}. The change magnitudes of $P(0, 0, z)$ are more obvious when $\sigma_{yy} < \sigma_{xx}$ than those when $\sigma_{yy} > \sigma_{xx}$. The changes in $\theta(0, 0, z)$ are just the reverse for $\sigma_{yy} > \sigma_{xx}$ and $\sigma_{yy} < \sigma_{xx}$. The value of $\varepsilon(0, 0, z)$ is a fixed one from the beginning to the end. The results obtained in the present paper will supply the theoretical basis and experimental evidence for the laser parameters selection when the electromagnetic GSM vortex beams propagate in biological tissues, and will be useful for the development of tissue imaging.

Acknowledgements – This work was supported by the National Natural Science Foundation of China (Grant Nos. 61405136, 11547264 and 11647085), and the Applied Basic Research Foundation of Shanxi Province, China (Grant No. 201701D121011).

References

[1] XIE S., LI H., LU Z., *Overview of tissue optics*, Physics **27**(10), 1998, pp. 599–604.

[2] WANRONG GAO, *Determination of spatial correlation functions of refractive index of living tissue*, Journal of Microscopy 245(1), 2012, pp. 43–48.

[3] WANRONG GAO, *Effect of tissue structure on resolution of imaging systems*, Journal of Modern Optics 60(15), 2013, pp. 1290–1296.

[4] WOLF E., *Introduction to the Theory of Coherence and Polarization of Light*, Cambridge University Press, Cambridge, 2007.

[5] WESTPHAL V., HELL S.W., *Nanoscale resolution in the focal plane of an optical microscope*, Physical Review Letters 94(14), 2005, article ID 143903.

[6] SCHMITT J.M., KUMAR G., *Turbulent nature of refractive-index variations in biological tissue*, Optics Letters 21(16), 1996, pp. 1310–1312.

[7] WANRONG GAO, KOROTKOVA O., *Changes in the state of polarization of a random electromagnetic beam propagating through tissue*, Optics Communications 270(2), 2007, pp. 474–478.

[8] WANRONG GAO, *Changes of polarization of light beams on propagation through tissue*, Optics Communications 260(2), 2006, pp. 749–754.

[9] XIAOYING LIU, DAOMU ZHAO, *The statistical properties of anisotropic electromagnetic beams passing through the biological tissues*, Optics Communications 285(21–22), 2012, pp. 4152–4156.

[10] JIAN WANG, *Advances in communications using optical vortices*, Photonics Research 4(5), 2016, pp. B14–B28.

[11] LEONHARD N.D., SHATOKHIN V.N., BUCHLEITNER A., *Universal entanglement decay of photonic-orbital-angular-momentum qubit states in atmospheric turbulence*, Physical Review A 91(1), 2015, article ID 012345.

[12] ZHIGANG ZHANG, FENGLIANG DONG, KEMAO QIAN, QINGCHUAN ZHANG, WEIGUO CHU, YUNTIAN ZHANG, XUAN MA, XIAOPING WU, *Real-time phase measurement of optical vortices based on pixelated micropolarizer array*, Optics Express 23(16), 2015, pp. 20521–20528.

[13] JINHONG LI, PENGHUI GAO, KE CHENG, MEILING DUAN, *Dynamic evolution of circular edge dislocations in free space and atmospheric turbulence*, Optics Express 25(3), 2017, pp. 2895–2908.

[14] JINHONG LI, JUN ZENG, *Dynamic evolution of coherent vortex dipole in atmospheric turbulence*, Optics Communications 383, 2017, pp. 341–348.

[15] JUN ZENG, JINHONG LI, *Dynamic evolution and classification of coherent vortices in atmospheric turbulence*, Optica Applicata 45(3), 2015, pp. 299–308.

[16] JINHONG LI, JUN ZENG, MEILING DUAN, *Classification of coherent vortices creation and distance of topological charge conservation in non-Kolmogorov atmospheric turbulence*, Optics Express 23(9), 2015, pp. 11556–11565.

[17] MEILAN LUO, QI CHEN, LIMIN HUA, DAOMU ZHAO, *Propagation of stochastic electromagnetic vortex beams through the turbulent biological tissues*, Physics Letters A 378(3), 2014, pp. 308–314.

[18] KOROTKOVA O., SALEM M., DOGARIU A., WOLF E., *Changes in the polarization ellipse of random electromagnetic beams propagating through the turbulent atmosphere*, Waves in Random and Complex Media 15(3), 2005, pp. 353–364.

[19] JINHONG LI, WEIWEI WANG, MEILING DUAN, JINLIN WEI, *Influence of non-Kolmogorov atmospheric turbulence on the beam quality of vortex beams*, Optics Express 24(18), 2016, pp. 20413–20423.

[20] ANDREWS L.C., PHILLIPS R.L., *Laser Beam Propagation through Random Media*, SPIE Press, Bellingham, 2005.

[21] YURA H.T., *Mutual coherence function of a finite cross section optical beam propagating in a turbulent medium*, Applied Optics 11(6), 1972, pp. 1399–1406.

[22] GRADSHTEYN I.S., RYZHIK I.M., *Table of Integrals, Series and Products*, Academic Press, New York, 2007.

[23] XIAOLING JI, XIAOWEN CHEN, *Changes in the polarization, the coherence and the spectrum of partially coherent electromagnetic Hermite–Gaussian beams in turbulence*, Optics and Laser Technology 41(2), 2009, pp. 165–171.

[24] ROYCHOWDHURY H., KOROTKOVA O., *Realizability conditions for electromagnetic Gaussian Schell -model sources*, Optics Communications 249(4–6), 2005, pp. 379–385.

Received June 30, 2017
in revised form August 29, 2017